

## Exercise: concepts from chapter 9

Reading: Fundamentals of Structural Geology, Ch 9

1) Data from rock mechanical testing of the Shiiya shale (Laboratory name, XT) a Japanese sedimentary rock, are reported in non-SI units and given in terms of confining pressures,  $P_c$ , and differential strengths in compression,  $D_c$ , by Hoshino et al. (1972).

	$P_c$ (kgf/cm <sup>2</sup> )	$D_c$ (kgf/cm <sup>2</sup> )
Shiiya shale (XT)	1	1532
	500	2980
	1000	3899
	1500	4172
	2000	4704
	2500	5758
Maze sandstone (XC)	1	1150
	500	2980
	1000	4040
	1500	4310
	2000	5172

- Convert these data to SI units. Calculate the two unique principal stresses,  $\sigma_1 = \sigma_2$  and  $\sigma_3$ , associated with each failure state, based on the values of confining pressure and differential strength. Show how the differential strength and triaxial compressive strength are related to the principal stresses.
- Plot the strength data for the Shiiya shale in principal stress space. Determine the best fitting straight line to define this part of the failure surface and write down the equation for this line. Use the linear fit to the data and the Coulomb failure criterion to determine the uniaxial compressive strength,  $C_u$ , and coefficient of internal friction,  $\mu_i$ .
- Calculate the differential strength and the triaxial compressive strength for the Shiiya shale for conditions of confining pressure that would be found at 5 km depth. Suggest reasons why this value is different from the uniaxial compressive strength based upon your understanding of the microscopic mechanisms that operate to limit the load-carrying capacity of rock subject to confining pressure.

- d) Construct a line representing the lithostatic stress state on the graph from part b) of principal stress space with the failure surface for the Shiiya shale. Draw a path representing the stress state changes during the laboratory experiment. Draw a path that the stress state might have followed during burial and deformation to reach the differential strength at 5 km depth. Discuss possible effects of stress path on strength.
- e) Consider the strength of Shiiya shale in triaxial experiments as defined by the linear segment of the failure surface from part b) of this exercise. Plot six points on the failure surface in principal stress space that are the predicted triaxial strengths for confining pressures representative of 0, 1, 2, 3, 4, and 5 km depths with no pore fluid pressure. Using Terzaghi's principal subtract pore pressures of 0, 10, 20, 30, 40, and 50 MPa from the respective principal stresses to plot six points on a new failure surface for Shiiya shale with pore fluid pressure on the same graph. Note that these pore pressures are what you would expect for hydrostatic columns of water to depths of 0, 1, 2, 3, 4, and 5 km. Based on the new confining pressures, however, calculate the new representative depths for these tests and the corresponding depths to the top of the water table.

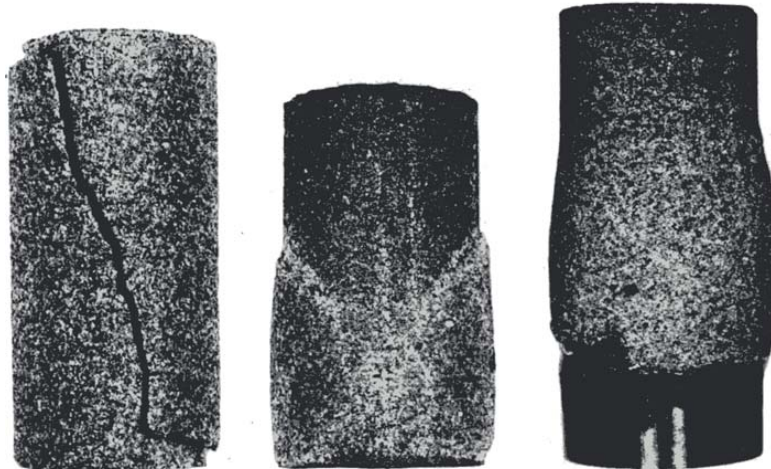


Figure 1. Photographs of Shiiya sandstone (SEF) specimens deformed at confining pressures of 0.1, 19.6, and 49.0 MPa from left to right. These show, respectively, an extension fracture, conjugate deformation bands, and bulging with no fracture. Note this is not the Shiiya shale (XT) (Hoshino et al., 1972).

2) Data from rock mechanical testing of the Maze sandstone (Laboratory name, XC) a Japanese sedimentary rock, are reported in non-SI units and given in terms of confining pressures,  $P_c$ , and differential strengths in compression,  $D_c$ , by Hoshino et al. (1972).

- a) Convert these data to SI units. Calculate the two principal stresses,  $\sigma_1$  and  $\sigma_3$ , associated with each failure state based on the values of confining pressure and differential strength. Plot these data in principal stress space.

- b) Use the best linear fit to these data as plotted in part a) and the Coulomb failure criterion to determine the uniaxial compressive strength,  $C_u$ , and coefficient of internal friction,  $\mu_i$ . Use these parameters to compute the inherent shear strength of the Maze sandstone. Write the Coulomb criterion for the Maze sandstone using these parameters.
- c) Recall that the Mohr diagram (Figure 6.23) is a plot of the magnitude of the shear stress (ordinate) versus the normal stress (abscissa). Plot the Coulomb criterion for the Maze sandstone on a Mohr diagram. Plot the five Mohr's half circles representing the stress states at failure from the laboratory test data. These half circles should be tangent to the line representing the Coulomb criterion if that is a good description of strength for this rock. Half circles that plot under this line would represent all possible pre-failure stress states. Because the linear Coulomb criterion does not necessarily correspond to laboratory data, Otto Mohr suggested that a smooth curve (now called the Mohr envelope) could be drawn tangent to the set of half circles from laboratory strength tests. Draw the Mohr envelope.
- d) In principle, the orientation of the shear fracture plane in a laboratory specimen should be given by the orientation of the line drawn from the center of a particular Mohr circle to the point where it touches the Mohr envelope. This line is oriented at the angle  $2\gamma_C$  to the abscissa, where  $\gamma_C$  is the angle between the direction of  $\sigma_1$  and the normal to the fracture plane. Construct such lines for the Maze sandstone deformed at 49 and 98 MPa confining pressures and determine the predicted orientation of the shear fracture. Compare your result to the shear fractures on the photographs from Hoshino et al., 1972 (Figure 2).

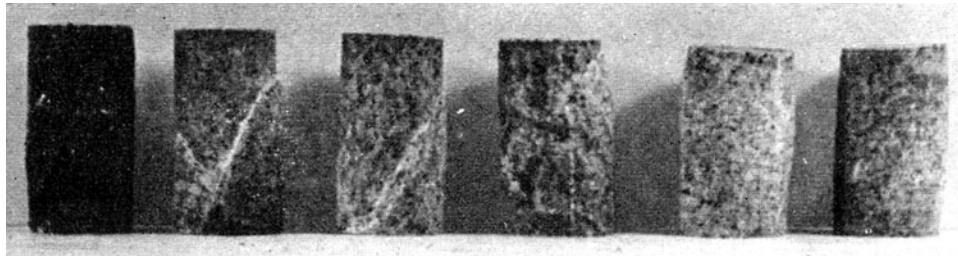


Figure 2. Photographs of Maze sandstone (XC) specimens deformed at confining pressures of 0.1, 49, 98, 147, 196, and 245 MPa from left to right. These show, respectively, wedge failure, single shear fracture, single shear fracture, network fracture, bulging with no fracture (Hoshino et al., 1972).

3) A. A. Griffith (1924) used different combinations of remote biaxial loading for the inclined elliptical hole (Figure 3) to investigate the growth of cracks from flaws in elastic solids. The distribution of tangential stress,  $\sigma_t$ , on the hole wall is given by (9.65). Note that there are the three applied loads (two remote principal stresses,  $\sigma_1$  and  $\sigma_3$ , and an internal pressure,  $P$ ) and three geometric parameters (half-length,  $a$ , half-width,  $b$ , and inclination angle,  $\beta$ ). Position around the hole is prescribed using the angle  $\eta$ . Because of the symmetry of this problem one only need consider the range  $-90^\circ \leq \eta \leq +90^\circ$ .

- a) Begin the analysis with the case of internal pressure of unit magnitude,  $P = 1$ , no remote stress, and a ratio  $a/b = 4$ . Systematically vary the inclination of the hole by changing the angle  $\beta$  from  $0^\circ$  to  $90^\circ$  in increments of  $15^\circ$  and plot the distributions of tangential stress versus position around the hole on the same graph so they can be compared. Explain why the stress distribution does not vary with inclination of the hole. Describe the distribution, noting the magnitude and position of the maximum and minimum tangential stress.

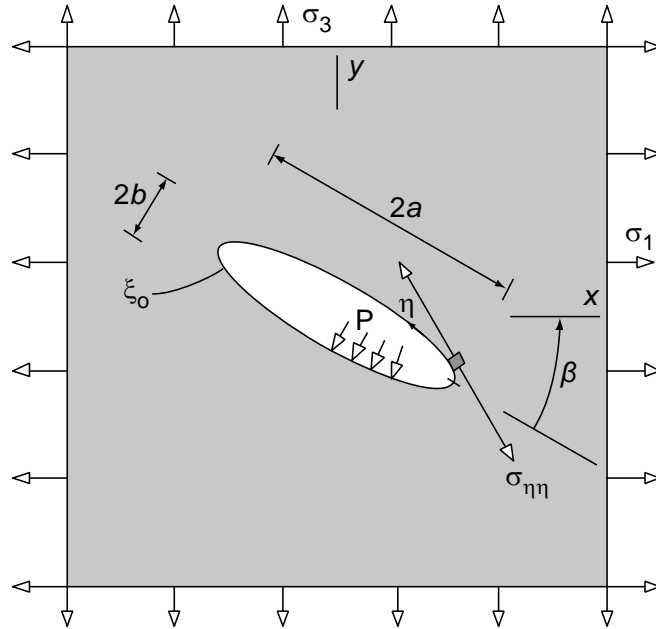


Figure 3. Schematic illustration of elastic boundary value problem for an inclined elliptical hole subject to biaxial remotely applied stress and internal pressure.

- b) Consider the case of a uniaxial remote tension of unit magnitude,  $\sigma_1 = 1$ , parallel to the  $x$ -axis, no internal pressure, and a ratio  $a/b = 4$ . Systematically vary the inclination of the hole (Figure 4) by changing the angle  $\beta$  from  $0^\circ$  to  $90^\circ$  in increments of  $15^\circ$  and plot the distributions of tangential stress versus position around the hole on the same graph so they can be compared. Describe how the stress distributions change with inclination.
- c) Griffith made the surprising discovery that the flaw could induce tensile stresses even though the applied stress is compressive. Impose a uniaxial remote compression of unit magnitude,  $\sigma_3 = -1$ , parallel to the  $y$ -axis and no internal pressure. Plot and describe the distribution of tangential stress on the hole boundary for different inclinations (Figure 4), varying the angle  $\beta$  from  $0^\circ$  to  $90^\circ$  in increments of  $15^\circ$ . Describe the range of  $\eta$  over which the tangential stress is tensile. What conclusions can you draw regarding the effects of inclination on the stress distribution? From the plot estimate the critical angle of inclination,  $\beta_c$ , at

which the tangential stress is greatest. Draw a sketch of the hole inclined at the critical angle and show where an opening fracture would initiate on the boundary and in what direction it would propagate. Use symmetry to determine where a second fracture would initiate and show its propagation direction.

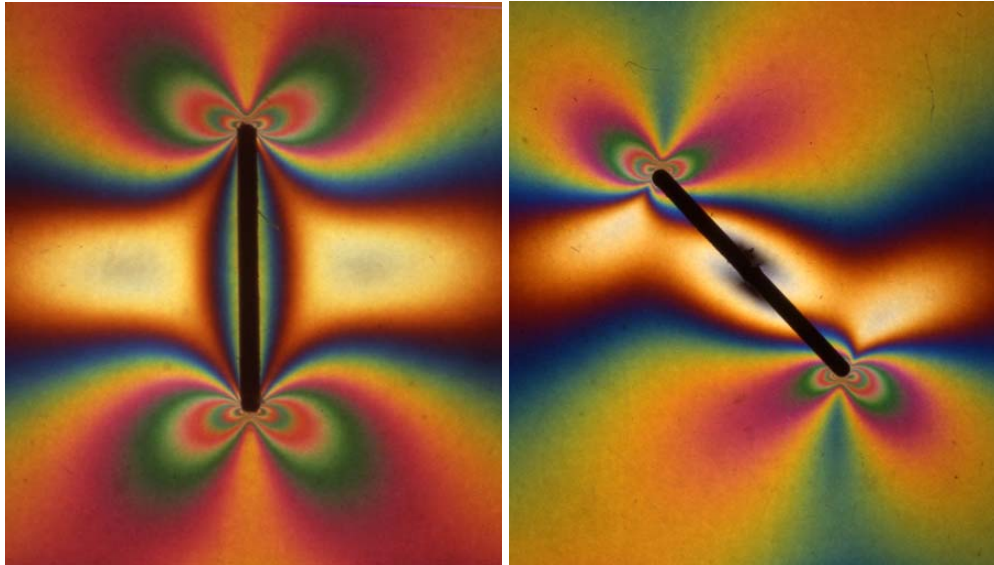


Figure 4. Photoelastic images of a narrow slot cut out of a plate subject to uniaxial tension. Colored bands are contours of the principal stress difference. The left slot is perpendicular to the direction of tension. The right slot is inclined to this direction.

- d) Investigate the effect of changing the shape of the cavity on the tangential stress. Impose a uniaxial remote compression of unit magnitude,  $\sigma_3 = -1$ , parallel to the  $y$ -axis and no internal pressure. Choose an inclination of  $\beta = 60^\circ$  and decrease the hole width,  $2b$ , in the sequence 0.40, 0.35, 0.30, 0.25, 0.20, 0.15, 0.10. Plot and describe how the distribution of tangential stress changes as the ratio of  $b$  to  $a$  decreases and the hole becomes more crack-like. Given this result and the result from part c) describe the shape and orientation of ‘most dangerous flaw’ in a rock mass subject to compression.

4) Fractures in rock are idealized as two adjacent, mirror image surfaces that are bounded in extent along a common curved line called the tipline. The direction of the displacement discontinuity between originally-adjacent points on these surfaces near the fracture tipline serves to classify fractures into three modes. (Figure 5). For mode-I fractures the displacement discontinuity is perpendicular to the fracture surfaces so they either open or close. Natural opening fractures include joints, veins, and dikes. In this exercise the near-tip mode-I stress field (9.72) is investigated to gain insights about the propagation of dikes and the associated damage zone.

- a) For a uniform remote normal stress,  $\sigma_{yy}^r$ , and a uniform normal stress at the fracture surfaces,  $\sigma_{yy}^c$ , the mode-I stress intensity factor is:

$$K_I = (\sigma_{yy}^r - \sigma_{yy}^c) \sqrt{\pi a} \quad (1)$$

For this loading state analyze the dimensions of the equations for the near-tip stress components and show that they are dimensionally homogeneous. Indicate the dimensions and units (S.I.) for the stress intensity factor.

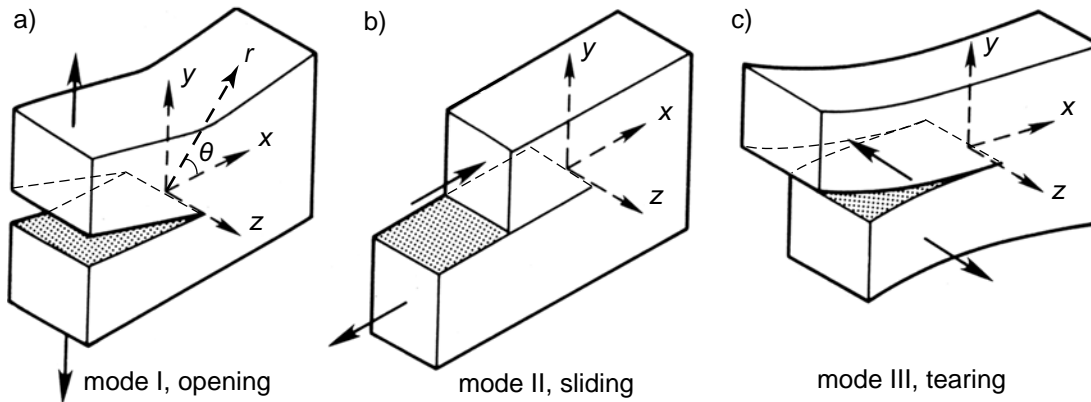


Figure 5. Three modes of fracture based upon near-tip displacement discontinuities (after Kanninen and Popelar, 1985). The fracture tipline lies along the  $z$ -axis and the fracture surfaces lie in the  $(x, z)$ -plane.

b) Calculate the Cartesian stress components for the near-tip stress field of the mode-I fracture. Recall that these functions are good approximations only for  $r < 0.01a$  where  $a$  is the half length of the fracture. Choose  $a = 1$  and  $K_I = 1$  and prepare contour plots of each component. Be sure to avoid the region very close to the tip. Describe these three stress distributions, commenting on how the sign and magnitudes of each component vary spatially. Rationalize the distribution of signs for the shear stress based on the kinematics of fracture opening.

c) Derive an equation for the maximum shear stress,  $\sigma_s$ , in the  $(x, y)$ -plane as a function of the Cartesian stress components for this plane strain problem. Calculate  $\sigma_s$  for the near-tip field and compare a contour plot of this stress with the photoelastic image in Figure 4a. Compare the distributions of  $\sigma_s$  and  $\sigma_{xy}$  (from part b) pointing out similarities and differences.

d) Figure 6 shows the distribution of ground cracks in Keanakakoi ash near a fissure that erupted from a dike on Kilauea volcano (also see Figure 9.32). Why did more than one crack form? Why are the cracks distributed to either side of the trace of the fissure? To address these questions suppose the cracks formed in the near-tip region of the dike as it approached the surface. Calculate the distributions of the normal stress components,  $\sigma_{xx}$  and  $\sigma_{yy}$ , about an opening fracture tip by plotting the appropriate functions of  $\theta$  from (9.72) versus the polar angle over the range,  $-\pi \leq \theta \leq +\pi$ . Describe these stress distributions and use them to predict the location and orientation of secondary fractures.



$$\begin{Bmatrix} \sigma_{rr} \\ \sigma_{\theta\theta} \\ \sigma_{r\theta} \end{Bmatrix} \cong \frac{K_I}{(2\pi r)^{1/2}} \begin{Bmatrix} \cos(\theta/2)[1 + \sin^2(\theta/2)] \\ \cos^3(\theta/2) \\ \sin(\theta/2)\cos^2(\theta/2) \end{Bmatrix} \quad (2)$$

The Polar coordinates  $(r, \theta)$  are defined in Figure 5a. Normalize the stress components so they are functions of  $\theta$  only and plot these versus the polar angle over the range  $-\pi \leq \theta \leq +\pi$ . Describe these stress distributions in terms of their symmetry, signs, and magnitudes. Discuss how the near-tip stress distribution might influence the direction of propagation.

b) To investigate the propagation of the kinked portion of the fracture calculate the distributions of the Polar stress components ( $\sigma_{rr}$ ,  $\sigma_{\theta\theta}$ , and  $\sigma_{r\theta}$ ) about a mode-II (sliding) fracture tip as given by Lawn and Wilshaw (1975):

$$\begin{Bmatrix} \sigma_{rr} \\ \sigma_{\theta\theta} \\ \sigma_{r\theta} \end{Bmatrix} \cong \frac{K_{II}}{(2\pi r)^{1/2}} \begin{Bmatrix} \sin(\theta/2)[1 - 3\sin^2(\theta/2)] \\ -3\sin(\theta/2)\cos^2(\theta/2) \\ \cos(\theta/2)[1 - 3\sin^2(\theta/2)] \end{Bmatrix} \quad (3)$$

These functions are for a right-lateral sense of sliding as illustrated in Figure 5b. Modify (3) to account for left-lateral sliding and to normalize the stress components as functions of  $\theta$  only. Plot the appropriate functions of  $\theta$  versus the polar angle over the range  $-\pi \leq \theta \leq +\pi$  and describe these stress distributions in terms of their symmetry, signs, and magnitudes. Discuss how this near-tip stress distribution might influence the direction of propagation.

c) Explain why the kinked portion of the fracture is so short relative to the main fracture trace. Predict what you would observe at the other end of the sheared joint if your explanation for the propagation mechanics is correct.